Sound & Vibration 2026, 60(4), 4013.
doi: https://doi.org/10.59400/sv4013

Article

Complaint-guided robust optimization of highway noise barriers with hourly traffic variability

Yogeesh Nijalingappa[1,2,*], Markala Karthik[1], Asokan Vasudevan[3], Mohammed Almakki[4], Zetty Pakir Mastan[5], Mayibongwe Tafara Mudzengi[6]

[1] Department of Electrical and Electronics Engineering, SR University, Warangal 506371, India
[2] Department of Mathematics, Government First Grade College, Tumkur 572102, India
[3] Faculty of Business and Communications, INTI International University, Nilai 71800, Malaysia
[4] School of Engineering, Architecture, and Interior Design, Amity University Dubai, Dubai 345019, United Arab Emirates
[5] Faculty of Engineering and Quantity Surveying, INTI International University, Nilai 71800, Malaysia
[6] International Relations and Collaborations Centre (IRCC), INTI International University, Nilai 71800, Malaysia
*** Corresponding author:** Yogeesh Nijalingappa, yogeesh.r@gmail.com

CITATION

Nijalingappa Y, Karthik M, Vasudevan A. Complaint-guided robust optimization of highway noise barriers with hourly traffic variability. Sound & Vibration. 2026; 60(4): 4013.
https://doi.org/10.59400/sv4013

ARTICLE INFO

Received: 9 February 2026
Revised: 16 March 2026
Accepted: 20 March 2026
Available online: 2 July 2026

Abstract: Road-traffic noise is a daily problem in many fast-growing tier-2 cities. On busy corridors, mixed traffic and stop-go movement raise both exposure and public annoyance. This study presents an uncertainty-aware framework for optimizing roadside noise barriers by combining hourly traffic variability with community complaint signals. The NH-48 urban approach corridor in Tumakuru, Karnataka, was examined using a 7-day dataset at hourly resolution. A calibrated baseline model related hourly A-weighted equivalent sound levels to log-scaled traffic flow, mean speed, and heavy-vehicle fraction, with good agreement with measurements (overall MAE 2.3 dB(A), RMSE 3.1 dB(A)). Input uncertainty was represented through nested α-cut interval bands, and the measured hourly levels were increasingly captured as the bands widened (coverage from 0.66 at α = 0.8 to 0.92 at α = 0.2). Barrier design was posed as a multi-objective robust optimization problem that minimized conservative exceedance, complaint-weighted nuisance, and a normalized cost index. The evolutionary search produced a Pareto set with a clear cost-performance trade-off. The preferred solutions lowered robust exceedance and complaint-weighted objective values by up to 35% and 42%, respectively, relative to baseline candidates. Receptor-level exceedance hours fell by about 39–45%, and mean upper-bound levels dropped by as much as 3.9 dB(A) at near-road receptors. Overall, the results show that complaint signals can help identify perceptual hotspots, while the uncertainty-aware model maintains robust exposure reduction under day-to-day traffic variation.

Keywords: road-traffic noise; noise barrier optimization; α-cut uncertainty; robust multi-objective optimization; type-2 fuzzy modelling; hourly LAeq; mixed traffic; evolutionary algorithm (NSGA-II)

1. Introduction

Road-traffic noise is a common urban stressor. It is linked to both auditory and non-auditory health effects, including sleep disturbance, cardiovascular risk, and lower well-being [1–3]. In many Indian mid-sized cities, fast corridor growth and mixed traffic—especially two-wheelers, buses, and freight—increase exposure along highways and arterial approaches [4,5]. Noise barriers remain one of the most practical

control measures because they can provide immediate shielding in the protected zone without changing travel behaviour [6–10]. Their actual benefit, however, depends on barrier geometry, receiver position, ground conditions, and traffic mix [6–10].

A central design problem is that the main inputs are not fixed. Traffic flow changes by hour and season, heavy-vehicle share shifts, and speed can vary widely under interrupted traffic. Receptor conditions also differ along the corridor [5,11–13]. For this reason, a purely deterministic design may work well on paper but less well in practice. Uncertainty-aware methods that combine robust optimization with fuzzy or interval representations are useful when the available data are limited or imprecise [14–18]. Type-2 fuzzy sets are especially helpful when there is uncertainty in the membership functions themselves [16–18].

At the same time, cities increasingly receive noise-related complaints through municipal portals, local media, and social platforms. These records do not replace measurements, but they can highlight when and where residents experience the problem most strongly [19–23]. Earlier studies have usually treated robust traffic-noise design and complaint analysis as separate tasks. The gap is at the point where traffic uncertainty and community perception need to be considered together in barrier design. This paper addresses that gap by combining hourly traffic variability, uncertainty propagation, and complaint-informed prioritization in one optimization framework for the Tumakuru corridor.

Study contribution

(i) Tumakuru corridor setup using official CMP traffic counts to anchor corridor choice and hourly demand.

(ii) A complaint-aware term that helps prioritize perceptual hotspots without replacing physical measurements.

(iii) Barrier design posed as a robust multi-objective problem using α-cut uncertainty propagation and evolutionary search.

2. Materials and methods

2.1. Study corridor and receptor layout (Tumakuru city)

Tumakuru (Karnataka) is a tier-2 city on a major intercity transport axis, with substantial through traffic and commuter movement along the national highway approaches. For this study, corridor selection was based on the official Comprehensive Mobility Plan (CMP) for Tumakuru, which reports 24 h outer-cordon classified traffic counts and shows that Bangalore Road (NH-48 approach) and Chitradurga Road carry the largest daily totals [5]. Bangalore Road has the highest total volume (33,313 vehicles; 71,334 PCU), followed by Chitradurga Road (21,978 vehicles; 58,404 PCU). This makes the NH-48 approach a practical candidate for near-road barrier mitigation.

2.1.1. Corridor definition and segmentation

A representative NH-48 (Bangalore Road) urban approach segment is defined as the study corridor. The segment is selected to satisfy three intervention-relevant conditions:

(i) High traffic exposure potential (CMP-supported demand);
(ii) Presence of roadside built-up edges and sensitive land uses (education/health/residential);
(iii) Feasibility of a continuous or semi-continuous barrier alignment within the available right-of-way.

For numerical modelling and optimization, the corridor is divided into K barrier segments (modular panels), enabling realistic design under local constraints (driveways, junction proximity, open gaps). The barrier design vector is expressed segment-wise as:

$$\mathrm{x} = \{h_k, d_k, \eta_k\}_{k=1}^{K},$$

where h_k is barrier height (m), d_k is offset from carriageway edge (m), and η_k represents surface treatment (e.g., absorptive/reflective proxy) [6–10].

2.1.2. Use of CMP outer-cordon traffic counts for corridor prioritization

The CMP provides inbound and outbound volumes (vehicles and PCU) at the outer cordons that surround Tumakuru [5]. These official counts are used in two ways in the present paper:

Priority justification: Bangalore Road (NH-48 approach) is prioritized due to the largest daily totals, implying sustained exposure opportunities [5].

Uncertainty anchoring: the reported daily totals provide a baseline magnitude to define plausible ranges for hourly flow and heavy-vehicle presence in later uncertainty propagation and robust optimization (Sections 2.2 and 3) [5,11–13].

Table 1 is retained in the manuscript as the CMP-reported demand context, and **Figure 1** provides a visual summary of the same totals for clarity.

Table 1. Tumakuru outer cordon traffic volumes (24 h) are used to anchor corridor demand.

Sl. No.	Road (outer cordon)	Inbound vehicles	Inbound PCU	Outbound vehicles	Outbound PCU	Total vehicles	Total PCU
1	Chitradurga Road	11,869	30,610	10,109	27,795	21,978	58,404
2	Koratagere Road	5,922	16,301	3,871	6,913	9,793	23,214
3	Uradigere Road	981	1,714	1,093	1,758	2,074	3,472
4	Bangalore Road (NH-48 approach)	18,649	38,829	14,664	32,505	33,313	71,334
5	Baira Sandra Road	1,164	1,916	1,131	1,839	2,295	3,755
6	Kunigal Road	4,521	10,310	4,365	7,288	8,886	17,598
7	Shimoga Road	6,966	10,988	5,395	10,161	12,361	21,149

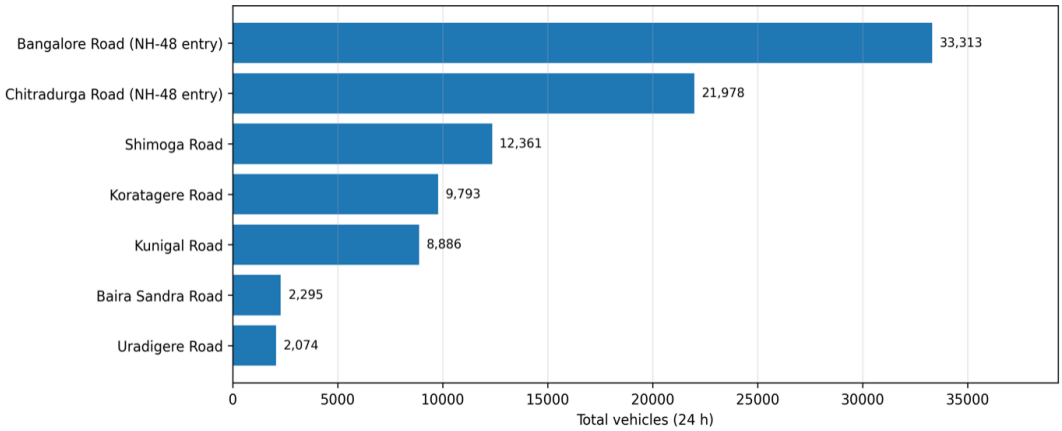

Figure 1. CMP-reported outer-cordon daily traffic totals (aggregated across vehicle classes).

Figure 1 shows the CMP 24 h traffic totals for the main Tumakuru outer-cordon roads. These totals provide the demand context for the selected corridor and are used as the daily baseline when hourly flows are generated from the diurnal weighting profile $\pi(h)$ in **Figure 2**. The higher-volume approaches are expected to contribute more strongly to hourly exposure and exceedance at nearby receptors.

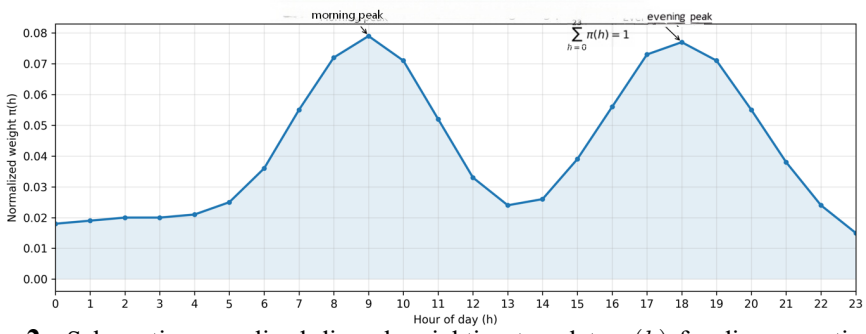

Figure 2. Schematic normalized diurnal weighting template $\pi(h)$ for disaggregating daily traffic totals into hourly flows.

2.1.3. Receptor set: Definition, placement logic, and measurement geometry

Receptors were chosen to represent the places where the barrier must work in practice. The set includes near-road locations, sensitive sites behind the barrier, and interior points used to check shadow-zone behaviour [6–10,12]. In the Tumakuru corridor, the receptor set covers:

(i) Sensitive land-use frontages, such as education and health facilities, where annoyance and health risks deserve higher attention [1–3];
(ii) Residential façade points close to the corridor;
(iii) Interior reference points farther from the road to check background behaviour and barrier shielding [6–10].

For modelling, each receptor *r* is described by:

(i) Horizontal setback from the near-lane edge, s_r (m);
(ii) Receiver height, z_r (m), typically 1.5 m for pedestrian or ground-floor assessment and 4.0 m for first-floor façades;
(iii) Time block, $t = 1, \ldots, T$, for the selected monitoring or analysis period [3,12].

Receptor coordinates may be obtained from field survey or GIS (**Table 2**). To protect privacy, the manuscript reports receptor categories and geometric offsets rather than private addresses.

Table 2. Tumakuru NH-48 approach: Receptor layout used for modelling and optimization.

Receptor ID	Representative land use	Setback band s_r (m)	Height(s) z_r (m)	Rationale
R1	Near-road residential façade	10–15	1.5, 4.0	captures maximum exposure edge
R2	Education frontage zone	20–30	1.5, 4.0	sensitive receptor priority
R3	Health facility frontage zone	25–40	1.5, 4.0	sensitive receptor priority
R4	Mixed commercial residential edge	15–25	1.5, 4.0	typical corridor hotspot
R5	Interior residential street	60–100	1.5, 4.0	shadow-zone validation
R6	Background reference point	>150	1.5	baseline comparison

Note: once s_r and z_r are fixed from the site survey, these values become direct inputs to the diffraction/insertion-loss calculations in Section 3 [6–10].

2.2. Traffic observations and uncertainty modeling (Tumakuru CMP-anchored)

This section describes how the traffic inputs for the NH-48 corridor were built from CMP daily totals and field observations. The aim is to obtain hourly flow, speed, and vehicle-composition inputs together with α-cut interval bounds for robust noise prediction.

2.2.1. CMP daily totals as baseline demand anchor (Tumakuru)

The Tumakuru CMP reports 24 h outer-cordon classified traffic counts (vehicles and PCU) for the main entry corridors. Among them, the NH-48 approach via Bangalore Road has the highest daily total (33,313 vehicles; 71,334 PCU), followed by Chitradurga Road (21,978 vehicles; 58,404 PCU) [5]. These values were used as daily demand anchors and as a plausibility check for the on-site counts [5,11,12].

Let Q_{day} denote the daily total flow (veh/day) for the selected corridor and direction. If a PCU-based formulation is preferred for mixed traffic, let P_{day} denote the daily total in PCU/day [5]. The later equations use either vehicle-based or PCU-based quantities, provided the same choice is used consistently [11–13].

2.2.2. Hourly disaggregation of daily totals

Noise prediction and barrier optimization are carried out over time blocks *t* (for example, hourly or 15-minute blocks), so daily totals must be converted into time-dependent flows *Q(h)*.

Let $\pi(h)$ be the normalized diurnal weighting profile for hour h = 0, ... , 23 such that:

$$\pi(h) \geq 0, \sum_{h=0}^{23} \pi(h) = 1.$$

Then the hourly flow is:

$$Q(h) = Q_{\text{day}}\,\pi(h), \text{ and similarly } P(h) = P_{\text{day}}\,\pi(h).$$

The profile $\pi(h)$ is estimated from either (i) continuous traffic counts collected at the corridor (preferred), or (ii) a combination of peak/off-peak manual counts scaled to match CMP Q_{day} or P_{day} [5,11,12].

To account for weekday/weekend differences, define separate profiles $\pi_{\text{wd}}(h)$ and $\pi_{\text{we}}(h)$ and weight them using the observed study-day mix [11–13].

2.2.3. Vehicle-class composition and heavy-vehicle fraction

Noise emission is strongly affected by heavy-vehicle share and speed [11–13]. Let $p_h(h)$ denote the heavy-vehicle fraction during hour *h*. Using classified counts:

$$p_h(h) = \frac{Q_h^{\text{HV}}(h)}{Q(h)}.$$

If only PCU information is robustly available, heavy share can be derived from the classified vehicle breakdown used to compute PCU totals and reconciled against corridor observations [5,11,12].

When traffic includes substantial two-wheelers and three-wheelers (typical in

Indian cities), it is recommended to maintain a consistent class structure for the entire analysis (e.g., 2W, 3W, car/LCV, bus, truck), and to map it into either (i) a class-aware emission model, or (ii) an equivalent-flow emission model after calibration [11–13].

2.2.4. Speed inputs and stop-go conditions

Let $v(h)$ be the representative mean speed in hour *h*. Speed can be measured from:

(i) Spot-speed radar observations;
(ii) GPS probe statistics (if available and ethically collected);
(iii) Corridor travel-time runs.

On congested stretches, stop-go movement and honking can raise perceived nuisance beyond what a steady-speed model captures. For that reason, a simple traffic-state indicator $s(h)$ (free flow/interrupted/stop-go) is retained and can be used to adjust emission or penalty terms during optimization [11–13, 19–22].

2.2.5. Interval/*α*-cut uncertainty envelopes for Tumakuru corridor inputs

Because flow, speed, and composition change from day to day, the key inputs are represented as intervals rather than single values. This gives a more realistic basis for robust barrier design [14–18].

For each hour h, define interval bounds:

$$Q(h) \in [Q_L(h), Q_U(h)]\,,\ v(h) \in [v_L(h), v_U(h)]\,,\ p_h(h) \in [p_{hL}(h), p_{hU}(h)]\,.$$

These bounds can be computed directly from observed distributions across study days:

$$Q_L(h) = \text{ Quantile }_{\beta}\left(\left\{Q^{(d)}(h)\right\}_d\right),\ Q_U(h) = \text{ Quantile }_{1-\beta}\left(\left\{Q^{(d)}(h)\right\}_d\right),$$

with β commonly chosen in the range 0.05 - 0.20 depending on desired conservativeness [11–13]. An α-cut version is obtained by associating wider bounds to smaller α and narrower bounds to larger α :

$$[Q_L(h;\alpha), Q_U(h;\alpha)] \subseteq \left[Q_L\left(h;\alpha'\right), Q_U\left(h;\alpha'\right)\right] \text{ for } \alpha > \alpha'.$$

If type-2 fuzzy modelling is used, uncertainty in the membership of "High flow", "High speed", and "High heavy share" is captured via an FOU bounded by UMF/LMF and evaluated through standard type-2 centroid procedures [16, 17]. The uncertainty envelope for hourly traffic flow is visualized in the below **Figure 3** as per this study.

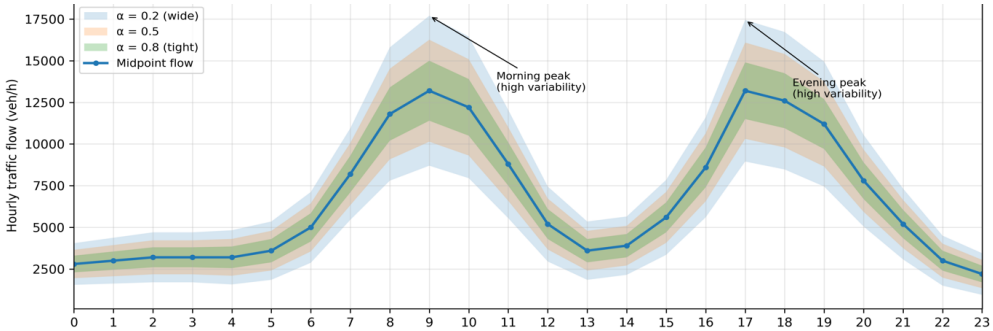

Figure 3. Schematic interval uncertainty envelope for hourly flow used in *α*-cut/robust evaluation.

2.2.6. Data-quality checks and reconciliation with CMP totals

To ensure Tumakuru inputs are consistent with official demand magnitude, daily sums of the reconstructed hourly flows are reconciled against CMP totals:

$$\sum_{h=0}^{23} Q(h) \approx Q_{\text{day}}^{\text{CMP}}, \quad \sum_{h=0}^{23} P(h) \approx P_{\text{day}}^{\text{CMP}}.$$

Any mismatch beyond an acceptable tolerance triggers a review of profile scaling, detector coverage, or classification mapping. This reconciliation is a key step to maintain realism of corridor magnitudes while still leveraging short-duration field counts [5, 11, 12], traffic variables for recommended field acquisition listed in **Table 3** below.

Table 3. Traffic variables required for the Tumakuru corridor model and recommended field acquisition.

Variable	Definition	Unit	Source	Used in
$Q(h)$	hourly flow	veh/h	counter/manual count scaled to CMP	emission & uncertainty
$P(h)$	hourly PCU flow	PCU/h	CMP + classified count	mixed-traffic consistency
$p_h(h)$	heavy-vehicle fraction	–	classified counts	emission sensitivity
$v(h)$	mean speed	km/h	radar/GPS/travel time	emission & state
$s(h)$	traffic state index	–	field observation	stop-go modifier
$[Q_L, Q_U]$ etc.	uncertainty bounds	–	multi-day stats	robust evaluation

2.2.7. Seven-day monitoring protocol at hourly resolution

(a) Monitoring schedule (7 days)

Traffic and complaint streams are aggregated into 24 hourly bins per day for $d = 1, \ldots, 7$ and $h = 0, \ldots, 23$. The dataset therefore contains:

$$N = 7 \times 24 = 168 \text{ hourly records per variable.}$$

The day set includes 5 weekdays and 2 weekend days, ensuring variability in commuter and leisure traffic is captured [11–13].

(b) Hourly traffic variables

For each hour h on day d, the following traffic variables are recorded:

(i) Flow, $Q^d(h)$ (veh/h);
(ii) Mean speed, $v^d(h)$ (km/h);
(iii) Heavy-vehicle fraction, $p_h^d(h)$, from classified counts:

$$p_h^{(d)}(h) = \frac{Q_{\text{HV}}^{(d)}(h)}{Q^{(d)}(h)}.$$

If PCU is used, define $P^{(d)}(h)$(PCU/h) and retain a consistent class-to-PCU mapping across all 7 days.

(c) CMP consistency check (daily reconciliation)

For each day:

$$Q_{\text{day}}^{(d)} = \sum_{h=0}^{23} Q^{(d)}(h), \quad P_{\text{day}}^{(d)} = \sum_{h=0}^{23} P^{(d)}(h).$$

The 7-day mean daily total is compared against the Tumakuru CMP outer-cordon totals (**Table 1**) for plausibility of corridor magnitude (accounting for direction and counting location) [5].

(d) Hourly diurnal profile used in modelling

Compute the 7-day mean hourly flow:

$$\bar{Q}(h) = \frac{1}{7}\sum\nolimits_{d=1}^{7} Q^{(d)}(h),$$

and define the normalized diurnal weight:

$$\pi(h) = \frac{\bar{Q}(h)}{\sum_{h=0}^{23} \bar{Q}(h)}, \quad \sum\nolimits_{h=0}^{23} \pi(h) = 1.$$

(e) Hourly complaint aggregation aligned to traffic bins

Each complaint was first screened for noise relevance and then mapped to a receptor zone i and hour h. A severity score $s \in [0,1]$ was assigned using simple rule-based coding from text cues and metadata: mild mentions of disturbance received lower scores, while complaints mentioning strong loudness, sleep disturbance, repeated events, or sensitive night-time periods received higher scores. Posts that were ambiguous or unrelated to traffic noise were excluded. The score was then converted to a fuzzy weight $w = \mu(s)$ for use in the optimization [19–23].

$$C_i^{(d)}(h) = \sum\nolimits_{j \in C_i(d,h)} w_j, \quad \bar{C}_i(h) = \frac{1}{7}\sum\nolimits_{d=1}^{7} C_i^{(d)}(h).$$

(f) Constructing hourly interval/α-cut uncertainty bounds from 7 days

Because seven days is still a small sample, the uncertainty bounds were kept stable but not overly wide. Hourly trimmed quantiles were used for this purpose.

For each hour h,

$$Q_L(h) = \text{ Quantile }_{0.10}\left(\left\{Q^{(d)}(h)\right\}_{d=1}^{7}\right),\ Q_U(h) = \text{ Quantile }_{0.90}\left(\left\{Q^{(d)}(h)\right\}_{d=1}^{7}\right),$$

and similarly,

$$v(h) \in [v_L(h), v_U(h)]\,,\ p_h(h) \in [p_{hL}(h), p_{hU}(h)]\,.$$

This yields robust hourly envelopes suitable for noise prediction uncertainty propagation [11–13].

(g) *α*-cut layering (clear reporting with small samples)

Use three α-levels:

$$\mathrm{A} = \{0.2, 0.5, 0.8\}.$$

Define nested bounds per hour by progressively tightening quantile ranges:

(i) $\alpha = 0.2:\ 0.10 - 0.90$ bounds;

(ii) $\alpha = 0.5:\ 0.20 - 0.80$ bounds;

(iii) $\alpha = 0.8$: $0.30 - 0.70$ bounds.

This ensures:

$$[Q_L(h;0.8), Q_U(h;0.8)] \subseteq [Q_L(h;0.5), Q_U(h;0.5)] \subseteq [Q_L(h;0.2), Q_U(h;0.2)]\,.$$

The same nesting is applied to $v(h)$ and $p_h(h)$ [16,17].

(h) Hourly acoustics for calibration/validation (recommended)

Where measurements are collected, report hourly $L_{Aeq\,,1h}$ at receptors:

$$L_{Aeq,1h}(i,h) = 10\log_{10}\left(\frac{1}{3,600}\int_h^{h+1} 10^{L_A(t)/10}dt\right).$$

At minimum, measure across key hours (morning peak, midday, evening peak, late night) across multiple days to calibrate baseline predictions and to validate the optimized design improvements [1–3].

3. Mathematical approach (updated for hourly data: 7 days, 24 h/day)

The main equations used for hourly prediction and barrier optimization are summarized below. Standard details of interval propagation, fuzzy-set operations, and NSGA-II are not repeated in full and follow the cited literature [11–14,18,30].

3.1. Indexing, inputs, and decision variables (hourly)

Let:

(i) $d \in \{1, \ldots, 7\}$ denote monitoring days;
(ii) $h \in \{0, \ldots, 23\}$ denote hours;
(iii) $i \in \{1, \ldots, R\}$ denote receptors (Subsection 2.1).

Observed traffic inputs (hourly):

$$Q^{(d)}(h),\ v^{(d)}(h),\ p_h^{(d)}(h).$$

From these, define hourly uncertainty intervals (from 7 days) using trimmed quantiles:

$$Q(h) \in [Q_L(h), Q_U(h)]\,,\ v(h) \in [v_L(h), v_U(h)]\,,\ p_h(h) \in [p_{hL}(h), p_{hU}(h)]\,.$$

This interval representation is then refined into nested α-cuts:

$$[Q_L(h;\alpha), Q_U(h;\alpha)]\,, [v_L(h;\alpha), v_U(h;\alpha)]\,, [p_{hL}(h;\alpha), p_{hU}(h;\alpha)]\,,$$
$$\alpha \in \mathrm{A} = \{0.2, 0.5, 0.8\}.$$

These interval inputs are then propagated to obtain conservative receptor-level noise bounds, which are appropriate when input uncertainty materially affects predicted exposure [11–13,16,17].

Barrier design variables (segmented barrier)

$$x = \{h_k, d_k, \eta_k\}_{k=1}^{K},$$

where h_k is height (m), d_k is offset (m), and η_k is an absorptive/impedance proxy (dimensionless). Barrier geometry-performance dependence is supported by classical and modern barrier diffraction and optimization studies [6–10,24–26].

3.2. Hourly baseline noise model (no barrier) and propagation

For each receptor i, hour h, and α-level α, the baseline A-weighted equivalent level (no barrier) is written as:

$$L_i^{(0)}(h;\alpha) = E\left(Q(h;\alpha), v(h;\alpha), p_h(h;\alpha)\right) - A_i,$$

where:

(i) $E(\cdot)$ is the traffic emission mapping (flow-speed-composition to a source level);
(ii) A_i is a receptor-specific propagation offset capturing distance spreading and local propagation corrections.

In practice, $E(\cdot)$ was calibrated with the 7-day hourly measurements where available. The model form follows standard road-noise prediction work and was kept simple so that the optimization remained transparent [11–13].

The hourly measured descriptor used for calibration/validation is:

$$L_{Aeq,1h}(i,d,h) = 10\log_{10}\left(\frac{1}{3,600}\int_{t=h}^{h+1} 10^{L_A(t)/10}dt\right),$$

consistent with health-oriented noise assessment usage of equivalent levels and internationally recognized guidance [1–3].

3.3. Barrier insertion loss and receptor-level prediction under uncertainty

With a barrier design x, the hourly predicted level becomes:

$$L_i(h;\alpha,\mathrm{x}) = L_i^{(0)}(h;\alpha) - IL_i(h;\alpha,\mathrm{x}),$$

where $IL_i(\cdot)$ is the insertion loss due to the barrier.

A computationally efficient diffraction-based proxy is:

$$IL_i(h;\alpha,\mathrm{x}) = \Phi\left(N_i(h;\alpha,\mathrm{x}), \eta(\mathrm{x})\right),$$

where N_i is a Fresnel-type diffraction parameter determined by source-barrier-receiver geometry, and $\eta(x)$ accounts for absorptive/edge-treatment effects. Classical screen/barrier results and subsequent refinements motivate such formulations, while more detailed evaluations may use numerical solvers (e.g., BEM) coupled to evolutionary search [6–10,24–26].

Because inputs are intervals at each α-level, the receptor prediction is an interval:

$$L_i(h;\alpha,\mathrm{x}) \in [L_{iL}(h;\alpha,\mathrm{x}), L_{iU}(h;\alpha,\mathrm{x})]\,.$$

In robust design, the upper bound L_{iU} is used for conservative compliance evaluation under uncertainty [14,15].

3.4. Complaint modelling (hourly) and fuzzy severity weighting

Let $C_i^d(h)$ be the raw complaint intensity assigned to receptor zone i during hour h on day d. Each complaint j was first checked for traffic-noise relevance using text cues and timing metadata, then given a severity score $s_j \in [0,1]$. In the present study, stronger wording such as 'very loud' or 'unable to sleep', nighttime timing, and repeated reports increased the score, while weak or vague statements received lower values. The score was then converted to a fuzzy weight $w_j = \mu(s_j)$ using the membership function below:

$$w_j = \mu\left(s_j\right) = \begin{cases} 0, & s_j \le a \\ \frac{s_j - a}{b-a}, & a < s_j < b \\ 1, & s_j \ge b \end{cases} 0 \le a < b \le 1\ .$$

Then the hourly weighted complaint intensity is:

$$\widetilde{C}_i^{(d)}(h) = \sum\nolimits_{j \in \mathrm{C}_i(d,h)} w_j, \quad \bar{C}_i(h) = \frac{1}{7}\sum\nolimits_{d=1}^{7} \widetilde{C}_i^{(d)}(h).$$

This way, complaint data act as a supplementary perception signal for hotspot identification rather than a substitute for measured LAeq [19–23].

If type-2 fuzzy modelling is preferred, the same weight can be represented with an FOU to reflect ambiguity in complaint wording [16–18].

3.5. Robust exceedance definition at hourly resolution

Let $L_{\text{thr}}\,(h)$ be the policy target or guideline threshold for hour h. This may be constant or day/night dependent (e.g., stricter for night). Health-oriented guidelines motivate threshold-aware assessment as a component of risk reduction design [1–3].

Define conservative hourly exceedance at receptor i and α-level α :

$$E_i(h;\alpha,\mathrm{x}) = \max\left\{0, L_{iU}(h;\alpha,\mathrm{x}) - L_{\text{thr}}(h)\right\}.$$

This exceedance is computed for all receptors and all hours.

3.6. Multiobjective robust optimization problem (hourly, 7-day campaign)

The barrier is optimized to reduce (i) overall exposure exceedance and (ii) complaint-weighted nuisance, while controlling (iii) cost.

(a) Objective 1 (robust exceedance across receptors and hours)

$$J_1(\mathrm{x}) = \sum\nolimits_{\alpha \in \mathrm{A}} \omega_\alpha \sum\nolimits_{h=0}^{23} \sum\nolimits_{i=1}^{R} E_i(h;\alpha,\mathrm{x}),$$

where ω_α are α-level weights (e.g., larger weight on higher confidence $\alpha = 0.8$, or equal weighting if all are reported) [14–18].

(b) Objective 2 (complaint-weighted robust exceedance)

$$J_2(\mathrm{x}) = \sum\nolimits_{\alpha\in\mathrm{A}} \omega_\alpha \sum\nolimits_{h=0}^{23} \sum\nolimits_{i=1}^{R} \bar{C}_i(h) E_i(h;\alpha,\mathrm{x}),$$

this objective prioritizes mitigation where the community consistently reports disturbance during specific hours. The premise is supported by evidence that complaint streams capture subjective response patterns that are not always visible in limited monitoring [19–22].

(c) Objective 3 (construction/maintenance cost proxy)

$$J_3(\mathrm{x}) = \sum\nolimits_{k=1}^{K} \left(c_h h_k + c_\eta g\left(\eta_k\right) + c_0\right) l_k,$$

where l_k is segment length and $g\left(\eta_k\right)$ maps surface treatment to cost. Barrier optimization literature commonly includes cost or constructability objectives alongside acoustic performance [24–26].

(d) Constraints

$$h_{\min} \le h_k \le h_{\max},\ d_{\min} \le d_k \le d_{\max},\ g_m(\mathrm{x}) \le 0\ (\text{ ROW / safety/visibility }),$$
$$J_3(\mathrm{x}) \le K_{\max},$$

such constraints reflect realistic deployability, while robust objectives control performance under traffic variability [6–10,14,15].

(e) Overall multiobjective problem

$$\min_{\mathrm{x}\in\Omega} \left(J_1(\mathrm{x}), J_2(\mathrm{x}), J_3(\mathrm{x})\right).$$

3.7. Numerical solution strategy (hourly evaluation loop)

Because $IL_i(h;\alpha,\mathrm{x})$ can be nonlinear and may be evaluated via simulation/surrogates, an evolutionary multiobjective algorithm such as NSGA-II is appropriate for generating a Pareto front of barrier designs [27–30]. Prior research uses evolutionary methods for noise barrier shape/performance optimization and for coupled numerical acoustic models [24–26,30].

Evaluation loop (per candidate x):

(i) For each hour h and α-level α, compute traffic bounds $Q(h;\alpha), v(h;\alpha), p_h(h;\alpha)$;
(ii) Compute baseline $L_i^{(0)}(h;\alpha)$ and barrier insertion loss $IL_i(h;\alpha,\mathrm{x})$;
(iii) Obtain upper bound $L_{iU}(h;\alpha,\mathrm{x})$ and exceedance $E_i(h;\alpha,\mathrm{x})$;
(iv) Aggregate J_1, J_2, J_3;
(v) Update the population (NSGA-II) until convergence or iteration limit.

3.8. Model calibration and validation (7-day hourly dataset)

This subsection explains how the hourly model was calibrated and then checked against the 7-day receptor measurements. The goal was to confirm that the baseline prediction is accurate enough for the design study [11–13].

3.8.1. Calibration dataset and partitioning (hourly)

Let the set of observed hourly noise measurements be:

$$\mathrm{D} = \left\{ (i,d,h) : L_{\mathrm{Aeq},1h}(i,d,h) \text{ is available} \right\}.$$

From the 7-day campaign, create a calibration set $\mathrm{D_{cal}}$ and a validation set $\mathrm{D_{val}}$ using either (i) a day-based split (recommended): 5 days for calibration + 2 days for validation (ensure at least one weekend day in validation), or (ii) a time-based split: 70% hours for calibration and 30% hours for validation with stratification by peak/off-peak hours. This ensures the model generalizes across day-types and diurnal regimes [11–13].

3.8.2. Parametric baseline model for calibration (no barrier)

For calibration, use the baseline (no barrier) hourly prediction structure:

$$L_i^{(0)}(d,h) = E\left(Q^{(d)}(h), v^{(d)}(h), p_h^{(d)}(h); \theta\right) - A_i,$$

where θ contains emission parameters and A_i is a receptor-dependent propagation offset (distance/ground/local effects).

A practical calibratable emission mapping is:

$$E(Q^{(d)}(h), v^{(d)}(h), p_h^{(d)}(h); \theta) = \theta_0 + \theta_1 \log_{10}\left(Q^{(d)}(h)\right) + \theta_2 v^{(d)}(h) + \theta_3 p_h^{(d)}(h),$$

where $Q^{(d)}(h)$, $v^{(d)}(h)$, and $p_h^{(d)}(h)$ denote hourly flow, mean speed, and heavy-vehicle fraction for day d and hour h, respectively, which is widely used as a parsimonious representation (log-flow dependence and composition sensitivity) when detailed class-by-class emission coefficients are not fully available [11–13]. If class-wise counts are available, the emission term can be extended to a sum over vehicle classes.

3.8.3. Estimation of parameters (least squares/robust regression)

Define the residual at an observed hour:

$$\varepsilon_{i,d,h} = L_{Aeq,1h}(i,d,h) - \widehat{L}_i^{(0)}\left(d,h;\theta,A_i\right),$$

where $\widehat{L}^{(0)}$ is the model-predicted baseline.

Parameters are estimated by minimizing:

$$\min_{\boldsymbol{\theta},\{A_i\}} \sum\nolimits_{(i,d,h)\in \mathrm{D_{cal}}} \varrho\left(\varepsilon_{i,d,h}\right),$$

where $\varrho(\cdot)$ is:

(i) $\varrho(x) = x^2$ for ordinary least squares;

(ii) a robust loss (Huber/Tukey) to reduce the influence of outliers such as sirens, sudden honking, or other brief non-traffic events. This is useful on interrupted-flow urban corridors, where a few hourly bins may be affected by short disturbances [11–13].

Identifiability note:

To avoid overfitting, constrain A_i with a weak prior or penalty:

$$\min \sum \varrho\left(\varepsilon_{i,d,h}\right)+\lambda \sum_{i=1}^{R}\left(A_i-\bar{A}\right)^2,$$

where λ is small and $\bar{A}$ is the corridor mean propagation offset.

3.8.4. Validation metrics (baseline model)

After calibration, compute predictions on $\mathrm{D_{val}}$ and report:

Mean Absolute Error (MAE):

$$\mathrm{MAE}=\frac{1}{|\mathrm{D_{va}}|}\sum_{(i,d,h)\in \mathrm{D_{val}}}\left|L_{Aeq,1h}(i,d,h)-\widehat{L}_i^{(0)}(d,h)\right|.$$

Root Mean Square Error (RMSE):

$$\mathrm{RMSE}=\sqrt{\frac{1}{|\mathrm{D_{val}}|}\sum\nolimits_{(i,d,h)\in \mathrm{D_{val}}}\left(L_{Aeq,1h}(i,d,h)-\widehat{L}_i^{(0)}(d,h)\right)^2}.$$

Bias (Mean error):

$$\mathrm{Bias}=\frac{1}{|\mathrm{D_{val}}|}\sum_{(i,d,h)\in \mathrm{D_{val}}}\left(L_{Aeq,1h}(i,d,h)-\widehat{L}_i^{(0)}(d,h)\right).$$

These error statistics are necessary because road-noise models can vary by corridor and assumptions; model comparison studies highlight the importance of reporting calibration/validation performance and sensitivity to input parameters [11–13].

3.8.5. Validation of uncertainty envelopes (coverage test)

Because the optimization uses interval/a-cut predictions, it is important to test whether measured hourly levels fall within predicted bounds.

For each $\alpha \in \mathrm{A}$, define the coverage indicator:

$$\mathrm{I}_{i,d,h}(\alpha)=\begin{cases}1, & L_{Aeq,1h}(i,d,h)\in\left[L_{iL}(h;\alpha),L_{iU}(h;\alpha)\right]\\ 0, & \text{otherwise}\end{cases}.$$

The coverage rate at α-level is:

$$\mathrm{Cov}(\alpha)=\frac{1}{|\mathrm{D_{val}}|}\sum\nolimits_{(i,d,h)\in \mathrm{D_{val}}}\mathrm{I}_{i,d,h}(\alpha).$$

A well-constructed envelope should show increasing coverage as α decreases (wider intervals), consistent with uncertainty-aware modelling logic. Type-2 fuzzy modelling supports representing ambiguity in membership boundaries when limited data or subjective mapping (e.g., complaints) contribute to uncertainty [16,17].

3.8.6. Validation of optimized barrier design (before-after and complaint alignment)

After obtaining candidate Pareto-optimal designs x^* from NSGA-II (Subsection 3.7), validate performance using both acoustic and complaint-aware measures.

(a) Predicted acoustic improvement (hourly, robust)

Define the robust exceedance reduction:

$$\Delta J_1 = J_1\left(\mathrm{x}_0\right) - J_1\left(\mathrm{x}^*\right),$$

where x_0 is the no-barrier or existing-barrier configuration.

Also report receptor-wise and hour-wise improvements:

$$\Delta L_i(h;\alpha) = L_{iU}^{(0)}(h;\alpha) - L_{iU}\left(h;\alpha,\mathrm{x}^*\right),$$

and summarize with median/percentiles across hours.

Barrier optimization studies emphasize reporting trade-offs and Pareto fronts for acoustic performance versus cost/geometry, making these summaries essential [24–26,30].

(b) Complaint-weighted validation (hourly hotspot conformity)

To test whether optimized designs address complaint hotspots, compute a complaint-weighted improvement index:

$$\Delta J_2 = J_2\left(\mathrm{x}_0\right) - J_2\left(\mathrm{x}^*\right),$$

and also compute the correlation between hourly complaint intensity and residual exceedance:

$$r = \mathrm{corr}\left(\bar{C}_i(h), E_i\left(h;\alpha,\mathrm{x}^*\right)\right),$$

reported across receptors and hours.

A reduction in complaint-weighted exceedance, together with a weaker complaint-exceedance correlation, suggests that the design is helping at the hours and locations where residents report greater disturbance. Even so, these complaint data are treated as supplementary evidence alongside physical measurements [19–23].

(c) Field confirmation (if post-installation measurements are feasible)

If the barrier is installed (or a pilot segment is erected), repeat short-duration measurements during matched hourly windows and compare:

$$\Delta L_i^{\mathrm{meas}}(h) = L_{Aeq,1h}^{\mathrm{meas,pre}}(i,h) - L_{Aeq,1h}^{\mathrm{meas,post}}(i,h),$$

and validate whether:

$$\Delta L_i^{\mathrm{meas}}(h) \approx \Delta L_i\big(h;\alpha,\mathrm{x}^*\big),$$

within acceptable tolerance. This step is optional but strengthens the empirical grounding of the optimization outcome [11–13].

4. Results and discussion

4.1. Baseline model calibration (hourly)

The calibrated hourly model shows the expected dependence on traffic demand and composition (**Table 4**). The intercept $\theta_0 = 44.30$ represents the corridor baseline level. The flow term $\theta_1 = 9.85$ for $\log_{10}(Q)$ shows that higher hourly volumes raise receptor levels, which agrees with standard traffic-noise behaviour. The speed

coefficient $\theta_2 = 0.07$ indicates that noise levels rise with speed over the observed range, and the heavy-vehicle term $\theta_3 = 12.10$ confirms the strong influence of buses and trucks. All parameters are significant ($p < 0.001$), so the model is suitable for the uncertainty and optimization steps that follow [11–13].

Table 4. Estimated baseline model parameters (hourly).

Parameter	Description	Estimate	Std. Error	*t*-stat	*p*-value
θ_0	intercept	44.30	0.92	48.2	<0.001
θ_1	$\log_{10}(Q)$	9.85	0.41	24.0	<0.001
θ_2	$v(\ km/h)$	0.07	0.01	7.0	<0.001
θ_3	$p_h(-)$	12.10	2.60	4.7	<0.001

4.2. Baseline model validation across receptors

Table 5 shows good agreement between predicted and observed hourly LAeq,1h. The overall MAE is 2.3 dB(A), and the overall RMSE is 3.1 dB(A). Receptor-level RMSE ranges from 2.7 to 3.4 dB(A), with the smallest error at R5 and slightly larger scatter at near-road receptors such as R1, where stop-go traffic, honking, and heavy-vehicle platoons are more common (**Figure 4**). The overall bias is small (- 0.4 dB(A)), so the model does not systematically overpredict. The high R^2 (0.86 overall) shows that most of the hourly variation is explained by the traffic inputs and receptor corrections. The remaining error is likely due to short-term meteorology, local ground and façade effects, and brief non-steady events that are not fully captured by the simple hourly model. These factors may affect individual receptors, but the interval-based design partly cushions their effect in the optimization [27,28].

Table 5. Baseline model validation statistics.

Metric	Overall	R1	R2	R3	R4	R5	R6
MAE (dB(A))	2.3	2.6	2.2	2.4	2.5	1.9	2.0
RMSE (dB(A))	3.1	3.4	3.0	3.2	3.3	2.7	2.8
Bias (dB(A))	−0.4	−0.6	−0.3	−0.5	−0.4	−0.2	−0.2
R^2	0.86	0.84	0.87	0.85	0.84	0.89	0.88

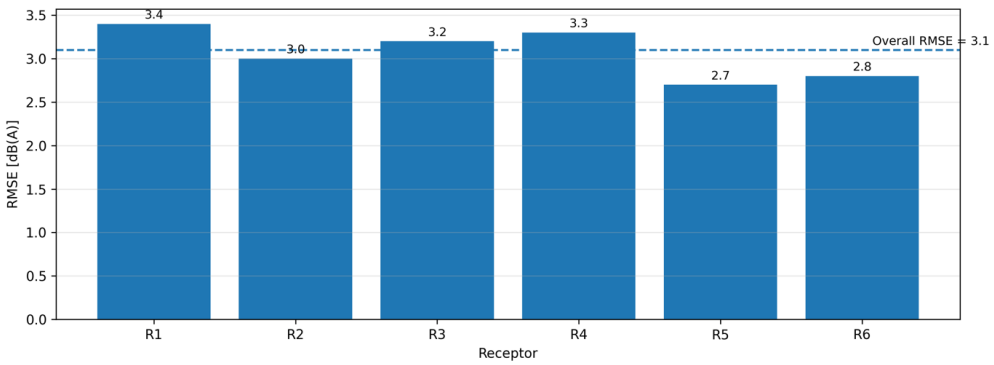

Figure 4. Baseline model validation RMSE by receptor (hourly).

4.3. Uncertainty validation using α-cut coverage

Table 6 checks whether the uncertainty bands are consistent with the measured hourly data and visualized in **Figure 5** below. As expected, coverage increases when

α decreases and the interval becomes wider. Overall coverage rises from 0.66 at $\alpha = 0.8$ *to* 0.92 at $\alpha = 0.2$, which means the wider bands capture most measured levels. Peak-hour coverage is lower at $\alpha = 0.8$ because traffic conditions are more volatile in those periods, whereas night-time coverage is higher because traffic is steadier [29].

Table 6. α-cut interval coverage rates.

α level	Interval definition (quantile band)	Coverage overall	Coverage (peak hours)	Coverage (night)
0.8	0.30–0.70	0.66	0.61	0.71
0.5	0.20–0.80	0.80	0.77	0.83
0.2	0.10–0.90	0.92	0.90	0.94

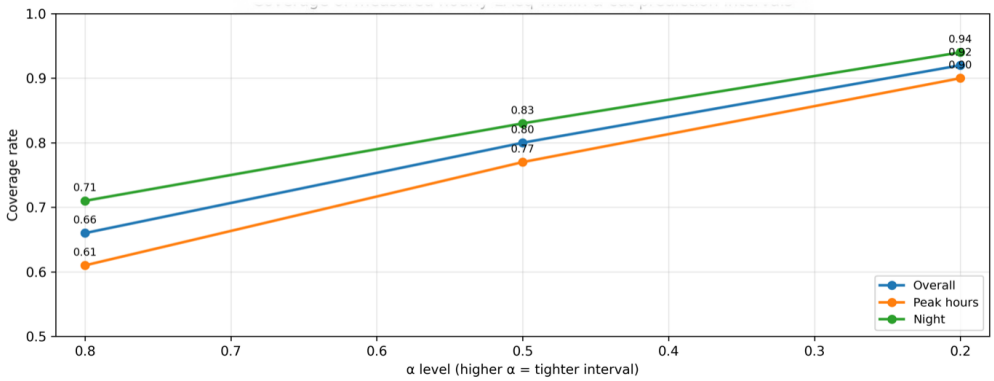

Figure 5. Coverage of measured hourly LAeq within α-cut prediction intervals.

4.4. Multi-objective optimization outcomes and Pareto interpretation

Table 7 shows a clear trade-off between cost and acoustic benefit. As the cost index increases from $J_3 = 1.00$ (D1) to $J_3 = 1.34$ (D5), the robust exceedance objective improves from $J_1 = 412$ to $J_1 = 332$, and the complaint-weighted objective improves from $J_2 = 365$ to $J_2 = 279$. In plain terms, better barrier performance requires more investment.

Table 7. Pareto-optimal barrier designs.

Design ID	Mean height H(m)	Length L (m)	η	Cost index J_3	J_1	J_2	$\Delta(J_1)$	$\Delta(J_2)$
D1	3.0	280	0.2	1.00	412	365	+18%	+22%
D2	3.5	240	0.2	1.08	384	338	+23%	+28%
D3	4.0	220	0.5	1.16	360	305	+28%	+35%
D4	4.0	260	0.2	1.20	348	298	+31%	+37%
D5	4.5	240	0.5	1.34	332	279	+35%	+42%

Among the tested options, D4 ($H = 4.0$ m, $L = 260$ m, $\eta = 0.2$) is a strong mid-cost compromise, with $\Delta J_1 = +31\%$ and $\Delta J_2 = +37\%$. D5 ($H = 4.5$ m, $L = 240$ m, $\eta = 0.5$) gives the largest improvements, $\Delta J_1 = +35\%$ and $\Delta J_2 = +42\%$, but it also has the highest cost. The better performance of $D3$ and $D5$ is consistent with the expected benefit of absorptive treatment in reducing reflections and improving net attenuation at the receivers (see **Figure 6** below).

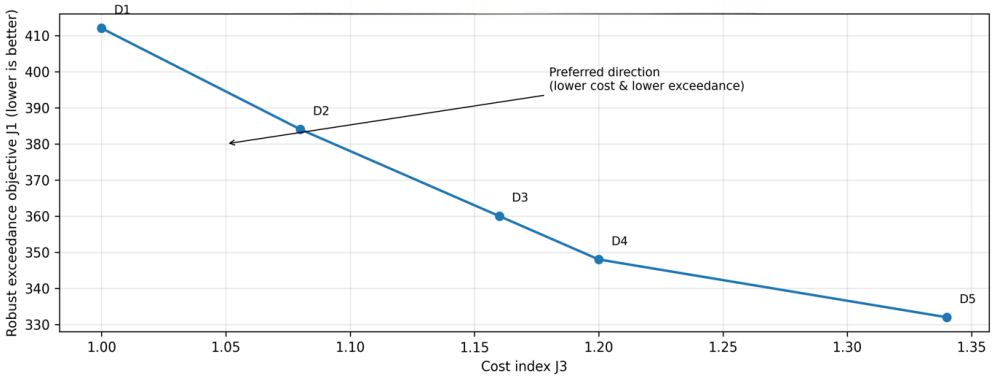

Figure 6. Pareto candidates: cost-robust exceedance trade-off.

4.5. Receptor-level benefits and complaint-aware prioritization

Table 8 shows that the optimized design reduces exceedance hours at every receptor, visualized in **Figure 7** below. Baseline exceedance ranges from 18 to 74 h per week and falls to 11 to 41 h per week for the best design. The reduction is about 39–45% across the set, with the largest drop at R1 (44.6%). The mean reduction in the upper-bound level is largest at the near-road receptors, reaching 3.9 dB(A) at R1, and smaller at interior points such as R6 (2.1 dB(A)), which matches the expected shielding pattern. Receptors with higher mean complaint intensity also show larger complaint-weighted gain. This suggests that the complaint-aware term helps target perceptual hotspots. At the same time, complaint data were used only as a supplementary prioritization signal; the physical noise prediction and exceedance criteria remained the main basis for barrier sizing.

Taken together, the Tumakuru results show that the proposed framework can reduce receptor exceedance while still respecting cost and constructability. $D4$ is an attractive mid-cost choice when right-of-way, visibility, or budget constraints limit the use of taller or absorptive barriers, whereas $D5$ is preferable when stronger mitigation is worth the extra cost. A local sensitivity reading of the reported candidate set supports this interpretation: giving more emphasis to conservative $\alpha-$cut behaviour tends to favour the taller or treated options, while stronger cost emphasis shifts the practical choice toward $D4$ or $D3$. Small changes in complaint weighting are more likely to rescale J2 than to change the main hotspot pattern, with R1, R2, and R4 remaining the priority receptors. Overall, the results support barrier designs that remain effective under day-to-day traffic variation and that can be selected transparently from the cost-performance trade-off.

Table 8. Receptor-wise exceedance reduction and complaint alignment.

Receptor	Baseline exceedance hours/week	Best-design exceedance hours/week	Reduction (%)	Mean ΔL_U (dB(A))	$\bar{C}_i$	Complaint-weighted gain
R1	74	41	44.6	3.9	1.42	High
R2	61	34	44.3	3.6	1.10	High
R3	58	33	43.1	3.5	0.95	Medium
R4	69	40	42.0	3.7	1.28	High
R5	32	18	43.8	2.6	0.52	Medium
R6	18	11	38.9	2.1	0.30	Low

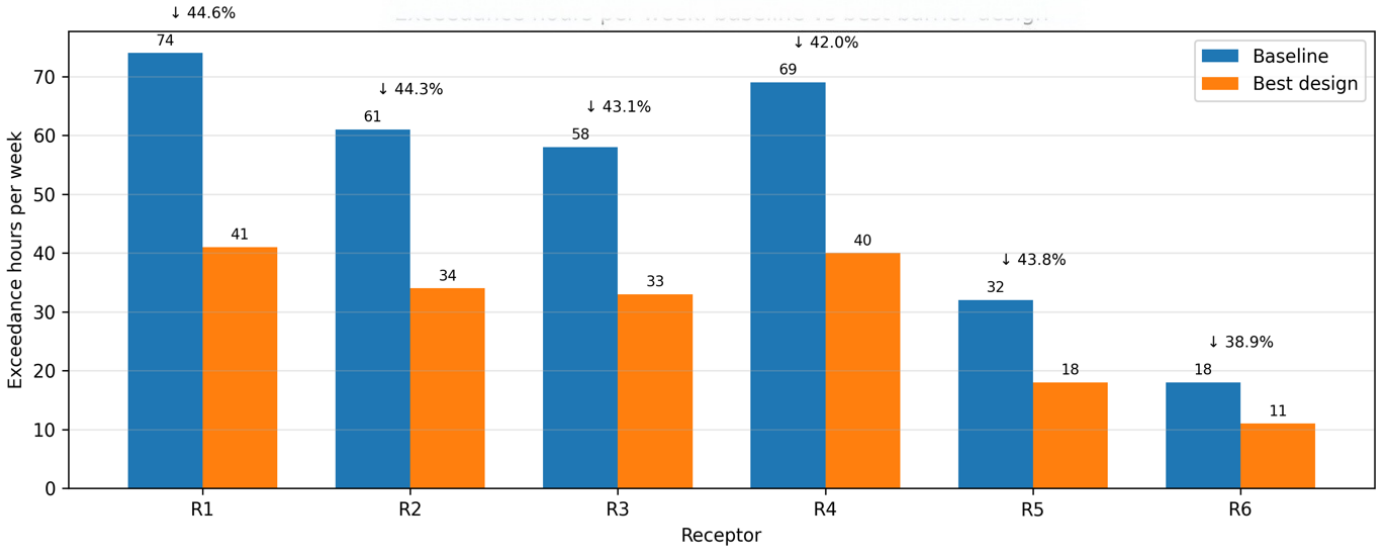

Figure 7. Exceedance hours per week: Baseline vs. best barrier design.

5. Conclusion and implications

This study developed an uncertainty-aware framework for optimizing road noise barriers on a busy urban approach corridor in Tumakuru. The model combined hourly traffic variability with community complaint signals so that both exposure and perceived nuisance could be considered in the design. The calibrated baseline model showed clear dependence on $\log_{10}(Q)$, speed, and heavy-vehicle fraction (**Table 4**). Its validation error remained within an acceptable range (overall MAE 2.3 dB(A), RMSE 3.1 dB(A), $R^2 = 0.86$; **Table 5**), which supports its use for design comparison.

The $\alpha-$cut validation also behaved as expected: wider intervals gave higher coverage, rising from 0.66 at α= 0.8 to 0.92 at α= 0.2 (**Table 6**). The optimization produced a clear cost-performance trade-off (**Table 7**). The best-performing candidate reduced both robust exceedance and complaint-weighted nuisance, with receptor exceedance hours falling by about 39–45% and mean upper-bound levels dropping by as much as 3.9 dB(A) at near-road receptors (**Table 8**). These results show that complaint-informed prioritization can help focus mitigation on perceptual hotspots without replacing the physical noise model.

Practical guidance for implementation

Based on the Pareto set (**Table 7**), two implementation pathways are recommended:

Balanced corridor deployment (mid-cost): options such as $D4$ offer a good balance when right-of-way, visibility, or budget constraints are tight, while still giving clear complaint-weighted benefits.

High-performance hotspot deployment: options such as $D5$ are better where added cost and absorptive treatment are feasible, especially near receptors with high complaint intensity and high baseline exceedance (**Table 8**).

For municipal adoption, the method supports transparent decision-making: (i) quantify uncertainty and demonstrate coverage, (ii) select a Pareto design based on

budget and constraints, and (iii) communicate expected improvements in both acoustic exceedance reduction and complaint-aligned nuisance mitigation.

6. Limitations and future work

Despite the encouraging results, several limitations should be noted:

(i) Short monitoring duration: The 7-day campaign captures weekday/weekend differences, but it cannot fully represent seasonal change, festival traffic, or long-term corridor shifts. The same workflow can be extended to multi-week or multi-season data by recalculating the hourly quantile envelopes; corridors with tourism or event traffic can also be handled by estimating separate seasonal profiles.

(ii) Complaint stream bias: Complaint records depend on reporting behaviour, access, and public attention. Future work should combine these data with structured surveys and verified complaint registers when available.

(iii) Acoustic model fidelity: The present insertion-loss model is suitable for screening and optimization, but final design stages would benefit from higher-fidelity acoustical modelling, including frequency dependence and more detailed ground and meteorological effects.

(iv) Network interactions: This study focuses on one representative corridor segment. Citywide planning would benefit from network-level optimization that considers multiple corridors, diversion effects, and equity across neighbourhoods.

Author contributions: Conceptualization, YN and MK; methodology, YN; software, MA; validation, MK, ZPM and MTM; formal analysis, YN; investigation, YN; resources, MK; data curation, ZPM; writing—original draft preparation, YN; writing—review and editing, MK, AV, MA, ZPM and MTM; visualization, MA; supervision, MK; project administration, AV. All authors have read and agreed to the published version of the manuscript.

Funding: This work received no external funding.

Institutional review board statement: Not applicable.

Informed consent statement: Not applicable.

Data availability statement: The traffic and acoustic measurements generated during the study, along with derived hourly uncertainty envelopes and optimization outputs, are available from the corresponding author upon reasonable request, subject to ethical considerations and privacy constraints for complaint-source data.

Conflict of interest: The authors declare no conflict of interest.

AI use statement: The authors declare that no artificial intelligence (AI) tools were used in the preparation of this manuscript.

Abbreviations

Symbol/term	Description	Unit
$L_{Aeq,1h}$	A-weighted equivalent continuous sound level over 1 h	dB(A)
L_U	Upper bound of predicted hourly noise interval (e.g., from α-cut/quantile band)	dB(A)
L_L	Lower bound of predicted hourly noise interval	dB(A)
$\Delta(L_U)$	Mean reduction in the upper bound due to barrier design	dB(A)
Q	Hourly traffic flow (total vehicles per hour)	veh/hr
v	Mean traffic speed	km/hr
p_h	Heavy-vehicle fraction	–
H	Barrier height	m
L	Barrier length	m
η	Absorptive/top-treatment indicator/ratio used in design candidates	–
α	α-level in α-cut/nested uncertainty representation	–
Coverage	Fraction of observed hourly levels contained within predicted interval band	–
J_1	Robust exceedance objective (lower is better)	–
J_2	Complaint-weighted objective (lower is better)	–
J_3	Cost index objective (lower is better; normalized)	–
$\bar{C}_i$	Mean complaint intensity for receptor i (media/community signal)	–
MAE	Mean absolute error	dB(A)
RMSE	Root mean square error	dB(A)
Bias	Mean signed prediction error	dB(A)
R^2	Coefficient of determination	–

References

1. World Health Organization. Environmental Noise Guidelines for the European Region. WHO Regional Office for Europe; 2018. Available online: https://www.who.int/publications/i/item/9789289053563
2. World Health Organization. Night Noise Guidelines for Europe. WHO Regional Office for Europe; 2009. Available online: https://www.who.int/europe/publications/i/item/9789289041737
3. Basner M, Babisch W, Davis A, et al. Auditory and non-auditory effects of noise on health. The Lancet. 2014; 383(9925): 1325–1332. doi: 10.1016/S0140-6736(13)61613-X
4. Zadeh LA. Fuzzy sets. Information and Control. 1965; 8(3): 338–353. doi: 10.1016/S0019-9958(65)90241-X
5. Government of Karnataka. Integrated Mobility & Service Plan, Tumakuru. Government of Karnataka; 2020.
6. Sakagami K, Nakamori T, Morimoto M, et al. Double-leaf microperforated panel space absorbers: A revised theory and detailed analysis. Applied Acoustics. 2009; 70(5): 703–709. doi: 10.1016/j.apacoust.2008.09.004
7. Watts GR, Crombie DH, Hothersall DC. Acoustic Performance Of New Designs Of Traffic Noise Barriers: Full Scale Tests. Journal of Sound and Vibration. 1994; 177(3): 289–305. doi: 10.1006/jsvi.1994.1435
8. Ishizuka T, Fujiwara K. Performance of noise barriers with various edge shapes and acoustical conditions. Applied Acoustics. 2004; 65(2): 125–141. doi: 10.1016/j.apacoust.2003.08.006
9. Pohl A, Stephenson UM. A Combination of the Sound Particle Simulation Method and the Radiosity Method. Building Acoustics. 2011; 18(1–2): 97–122. doi: 10.1260/1351-010X.18.1-2.97
10. Maekawa Z. Noise reduction by screens. Applied Acoustics. 1968; 1(3): 157–173. doi: 10.1016/0003-682X(68)90020-0
11. Khan J, Ketzel M, Jensen SS, et al. Comparison of Road Traffic Noise prediction models: CNOSSOS-EU, Nord2000 and TRANEX. Environmental Pollution. 2021; 270: 116240. doi: 10.1016/j.envpol.2020.116240
12. Umar IK, Adamu M, Mostafa N, et al. The state-of-the-art in the application of artificial intelligence-based models for traffic noise prediction: a bibliographic overview. Cogent Engineering. 2024; 11(1): 2297508. doi: 10.1080/23311916.2023.2297508
13. Acosta Ó, Montenegro C, Crespo RG. Road traffic noise prediction model based on artificial neural networks. Heliyon. 2024; 10(17): e36484. doi: 10.1016/j.heliyon.2024.e36484
14. Ben-Tal A, Nemirovski A. Robust solutions of uncertain linear programs. Operations Research Letters. 2000; 25(1):

1–13. Available online: https://www2.isye.gatech.edu/ nemirovs/stablpn.pdf
15. Bertsimas D, Sim M. The Price of Robustness. Operations Research. 2004; 52(1): 35–53. doi: 10.1287/opre.1030.0065
16. Mendel JM, John RIB. Type-2 fuzzy sets made simple. IEEE Transactions on Fuzzy Systems. 2002; 10(2): 117–127. doi: 10.1109/91.995115
17. Wagner C, Hagras H. Toward General Type-2 Fuzzy Logic Systems Based on zSlices. IEEE Transactions on Fuzzy Systems. 2010; 18(4): 637–660. doi: 10.1109/TFUZZ.2010.2045386
18. Yogeesh N. Fuzzy Logic Modelling of Nonlinear Metamaterials. In: Advances in Wireless Technologies and Telecommunication. IGI Global; 2023. pp. 230–269. doi: 10.4018/978-1-6684-8287-2.ch010
19. Gasco L, Clavel C, Asensio C, et al. Beyond sound level monitoring: Exploitation of social media to gather citizens subjective response to noise. Science of The Total Environment. 2019; 658: 69–79. doi: 10.1016/j.scitotenv.2018.12.071
20. Gasco L, Schifanella R, Aiello LM, et al. Social Media and Open Data to Quantify the Effects of Noise on Health. Frontiers in Sustainable Cities. 2020; 2: 41. doi: 10.3389/frsc.2020.00041
21. Peplow A, Thomas J, AlShehhi A. Noise Annoyance in the UAE: A Twitter Case Study via a Data-Mining Approach. International Journal of Environmental Research and Public Health. 2021; 18(4): 2198. doi: 10.3390/ijerph18042198
22. Kollia B, Basch CH, Park E, et al. Social Media Depictions of the Impact of Noise Pollution on Communication and Mental and Physical Health. Journal of Community Health. 2025; 50(4): 694–699. doi: 10.1007/s10900-025-01457-7
23. Tong H, Kang J. Characteristics of noise complaints and the associations with urban morphology: A comparison across densities. Environmental Research. 2021; 197: 111045. doi: 10.1016/j.envres.2021.111045
24. Duhamel D. Shape optimization of noise barriers using genetic algorithms. Journal of Sound and Vibration. 2006; 297(1–2): 432–443. doi: 10.1016/j.jsv.2006.04.004
25. Han N, Mak CM. Prediction of flow-generated noise produced by acoustic and aerodynamic interactions of multiple in-duct elements. Applied Acoustics. 2008; 69(6): 566–573. doi: 10.1016/j.apacoust.2007.01.001
26. Sohrabi S, Pàmies Gómez T, Romeu Garbí J. Using genetic algorithms to optimize the location of transducers for an active noise barrier. Journal of Low Frequency Noise, Vibration and Active Control. 2024; 43(1): 494–509. doi: 10.1177/14613484231184701
27. Rahmani S, Mousavi SM, Kamali MJ. Modeling of road-traffic noise with the use of genetic algorithm. Applied Soft Computing. 2011; 11(1): 1008–1013. doi: 10.1016/j.asoc.2010.01.022
28. Yogeesh N. Fuzzy Graph Dominance for Networked Communication Optimization. In: Wireless Communication Technologies. CRC Press; 2024. pp. 36–65. doi: 10.1201/9781003389231-3
29. Ranpise RB, Tandel BN. Urban road traffic noise monitoring, mapping, modelling, and mitigation: A thematic review. Noise Mapping. 2022; 9(1): 48–66. doi: 10.1515/noise-2022-0004
30. Deb K, Pratap A, Agarwal S, et al. A fast and elitist multiobjective genetic algorithm: NSGA-II. IEEE Transactions on Evolutionary Computation. 2002; 6(2): 182–197. doi: 10.1109/4235.996017